Dark solitary waves in 1D Bose-Einstein condensates

Author: Carlos Bravo Prieto

Facultat de Física, Universitat de Barcelona, Diagonal 645, 08028 Barcelona, Spain.

Advisor: Ricardo Mayol Sánchez

Abstract: We study the dynamical properties of 1D solitary waves in confined Bose-Einstein condesates of ultracold gases with repulsive interparticle interactions. We perform numerical simulations of the Gross-Pitaevskii equation for harmonically trapped systems in the presence of dark and grey solitons, and we compare them with analytical solutions derived for homogeneous condensates. Our numerical results show a very good agreement with the theory in the limit of large trapped systems, which are available in current experiments.

I. INTRODUCTION

In the last two decades, the phenomenon of Bose-Einstein condensation has become an increasingly active area of research, both experimentally and theoretically. A Bose-Einstein condensate is a state of matter that a bosonic system reaches below a certain critical temperature. The transition to this state occurs when the thermal de Broglie wavelength becomes comparable to the mean interparticle separation. When this condition is attained, a macroscopic fraction of the bosons occupies the lowest single-particle quantum state. The Bose-Einstein condensation plays remarkable roles in atomic, elementary particle, nuclear, condensed matter physics and astrophysics [1].

The prototype of a system of bosons undergoing Bose-Einstein condensation is the superfluid ^{4}He, but due to the strong interaction between helium atoms the condensate fraction, i.e. the ratio N_0/N between the number of condensed particles N_0 and the total number of particles N, is dramatically reduced. For this reason it is advisable to look for systems where the interaction between particles is weaker. Currently available systems that fulfill this condition are the Bose-Einstein condensates of ultracold gases (BECs). The first BECs made of alkali atoms were realized in 1995 by using powerful laser-cooling methods [2], providing unique opportunities for exploring quantum phenomena on a macroscopic scale. Due to the fact that in a BEC most of the atoms occupy the same quantum state, the condensate can be very well described in terms of a mean-field theory. This is the so-called Gross-Pitaevskii (GP) theory, which has reproduced with excellent agreement numerous experimental results, e.g. the nucleation and dynamics of quantized vortices, the manifestation of the Josephson effect in double well potentials or in spinor condensates, the superfluid response of the system against rotation, or the generation and motion of topological defects as solitons.

In this work we analyze the dynamical features of dark solitonic waves in harmonically trapped, 1D BECs with repulsive interatomic interactions. We start by characterizing the solitonic waves of this type in homogeneous systems, where dark solitons are one of the analytic solutions of the GP equation. Then, we perform numerical simulations for calculating the properties of dark solitons in trapped condensates, and discuss the matching of our results, in the limit of large trapped systems, comparing with the analytical properties derived from the homogeneous case. Additionally, we study the oscillatory motion of dark solitons in harmonic traps, and compare with the predictions of a classical equation of motion derived from the conserved energy of the soliton.

II. THEORY

The Gross-Pitaevskii theory is a mean-field approximation that provides a nonlinear Schrödinger equation for the wave function $\psi(\vec{r}, t)$ (also called the order parameter) of the condensate. It is valid when the s-wave scattering length a_s is much smaller than the average distance between atoms and the number of atoms in the dilute system becomes large enough [3] (as is usual in the mean-field theories). The time-dependent GP equation is [4]

$$i\hbar \frac{\partial}{\partial t}\psi = \left(-\frac{\hbar^2}{2m}\nabla^2 + V_{ext}(\vec{r}) + g|\psi|^2 \right)\psi \ , \qquad (1)$$

where $g = 4\pi\hbar^2 a_s/m$ is the interaction strength, $V_{ext}(\vec{r})$ is an external potential, and ψ is normalized to the total number of particles $\int d\vec{r}|\psi|^2 = N$.

For stationary solutions $\psi(\vec{r}, t) = \psi(\vec{r})\exp(-i\mu t/\hbar)$, where μ is the chemical potential, and the GP Eq. (1) becomes

$$\left(-\frac{\hbar^2}{2m}\nabla^2 + V_{ext}(\vec{r}) + g|\psi|^2 \right)\psi = \mu\psi \ . \qquad (2)$$

In the absence of interactions ($g = 0$) this equation reduces to the usual Schrödinger equation for the non-interacting hamiltonian. The energy of the system can be calculated from the functional [3]

$$E[\psi] = \int d\vec{r} \left[\frac{\hbar^2}{2m}|\nabla\psi|^2 + V_{ext}(\vec{r})|\psi|^2 + \frac{g}{2}|\psi|^4 \right] \ . \qquad (3)$$

Exact solutions: dark solitons

In the homogeneous case, $V_{ext}(\vec{r}) = 0$, the GP Eq. (1) has analytical solutions. One particular kind of these solutions are the so-called solitons [3]. A soliton is a solitary wave that propagates preserving its intrinsic shape, and can interact with other solitons emerging from the collision unchanged, except for a phase shift [5]. There are two different solitonic solutions: the bright soliton and the dark (grey) soliton. Both solutions correspond to a localized modulation of the density profile characterized by an increase (bright) or a suppression (dark, or grey if the supression is not total) of the density respect the bulk value. The typical length characterizing the extension of the density modulation is fixed by the healing length ξ.

If the interaction is attractive ($g < 0$), the solitonic solution to Eq. (2) corresponds to a bright soliton with functional form $\propto \operatorname{sech}(x/\sqrt{2}\xi)$ and negative chemical potential. This type of solitons can move freely in space (along the x-direction) like an ordinary particle. In spite of the fact that bright solitons are not stable configurations, they can be produced in traps with tight radial confinement, where the mechanism of destabilization is reduced [6].

We focus on the case of repulsive interparticle interactions ($g > 0$), where there exist an analytical solution to the GP Eq. (1) for a solitary wave moving with constant velocity v on a constant background [7]:

$$\psi_s = \sqrt{n} \left(i\frac{v}{c} + \sqrt{1 - \left(\frac{v}{c}\right)^2} \tanh\left[\frac{x - vt}{\sqrt{2}\xi} \sqrt{1 - \left(\frac{v}{c}\right)^2} \right] \right), \tag{4}$$

where n is the background (ground state) constant density, $c = \sqrt{gn/m}$ is the speed of sound and the healing length is given by $\xi = \hbar/\sqrt{2mgn}$. The density profile $n(x) = |\psi_s|^2$ has a minimum at the center of the soliton corresponding to $n(0) = nv^2/c^2$. Notice that for the static case ($v = 0$), i.e. the dark soliton, the minimum density is equal to zero. The width of the soliton is fixed by the healing length ξ and amplified by the factor $1/\sqrt{1 - (v/c)^2}$, which increases as v approaches c. The chemical potential is positive and is given by the background density where the condensate is living, $\mu = gn$.

In contrast to the bright soliton case, dark (and grey) solitons present topological features that deserve a further analysis. Dark solitons can be seen as topological defects connecting two ground states with the same density but different phase [8]. The phase S of the wave function $\psi(x) = \sqrt{n(x)}e^{iS(x)}$ undergoes a finite change as x varies from $-\infty$ to $+\infty$:

$$\Delta S = S(\infty) - S(-\infty) = 2\cos^{-1}\left(\frac{v}{c}\right) . \tag{5}$$

For a static dark soliton the phase change is given by $\Delta S = \pi$ and the wave function $\psi_s(x) = \sqrt{n}\tanh(x/\sqrt{2}\xi)$ is real.

Fig. 1 shows the characteristic density profiles (upper panel) and phases (lower panel) of moving grey solitons
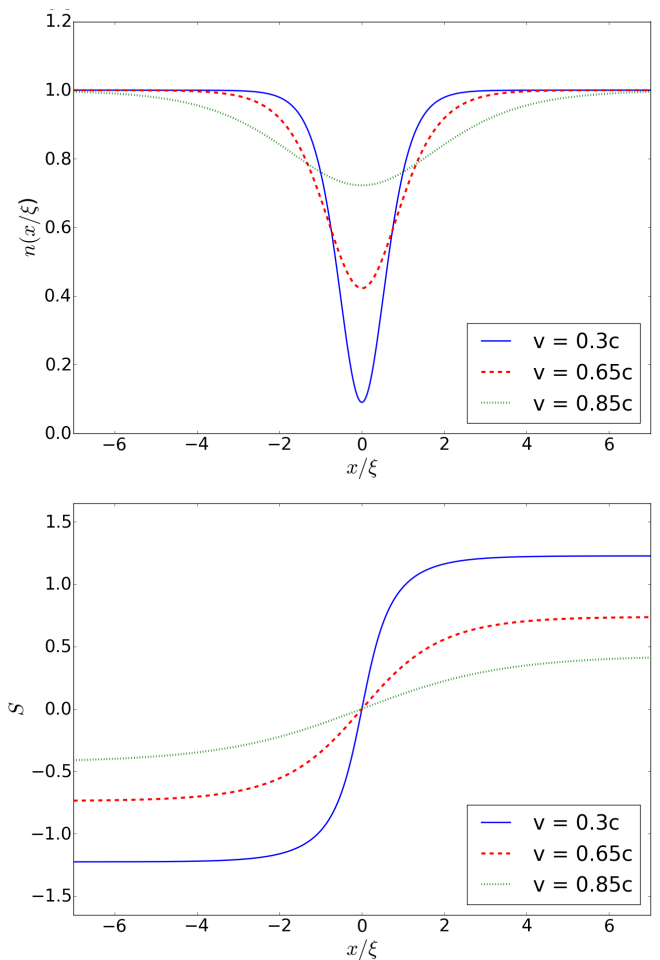

FIG. 1: Density profiles (upper panel) and phases (lower panel) of 1D moving grey solitons with varying velocity in an homogenous background with density $n = 1/\xi$.

with varying velocity. As can be seen, the width of the soliton, which is proportional to the healing length ξ, increases as v approaches c. On the other hand, the phase change ΔS increases up to π as v approaches zero.

The excitation energy ε_s of the soliton can be evaluated by taking the difference between the grand canonical energies (since the system is open) in the presence and in the absence of the soliton for fixed chemical potential $\varepsilon_S = (E[\psi_s] - \mu N) - (E[\psi_{GS}] - \mu N_{GS})$, where N and N_{GS} are the number of particles for the state with the soliton and for the ground state, respectively. The resulting expression is [9]

$$\varepsilon_S = \int_{-\infty}^{\infty} \left[\frac{\hbar^2}{2m} \left| \frac{d\psi_s}{dx} \right|^2 + \frac{g}{2}(|\psi_s|^2 - n)^2 \right] dx , \tag{6}$$

and can be easily calculated from Eq. (4). The result is

$$\varepsilon_S(\mu, v) = \frac{4}{3} \frac{\hbar m}{g} \left(\frac{\mu}{m} - v^2 \right)^{3/2} . \tag{7}$$

It is worth noticing that the velocity of the soliton in-

creases when its energy decreases. The main consequence is that the inertial mass of the soliton is negative

$$M_{in} = \frac{1}{v} \left. \frac{\partial \varepsilon_s}{\partial v} \right|_\mu < 0 \ . \qquad (8)$$

As $v \rightarrow c$ the excitation energy of the soliton approaches zero, and the nonlinear solitonic solution to the GP equation converges with the linear sound excitations (phonons) of the constant ground state.

The number of particles N_s depleted from the background density by the dark soliton can be evaluated from the difference between the number of particles in the presence and in the absence of the soliton for fixed chemical potential. The missing number of particles of the dark soliton is [9]

$$N_s = - \left. \frac{\partial \varepsilon_s}{\partial \mu} \right|_v = -\frac{2\hbar}{g} \sqrt{\frac{\mu}{m}} \ . \qquad (9)$$

The topological nature of dark solitons makes them dynamically stable states (i.e. stable in the absence of dissipation) against decay to the ground state of the system. However, they are unstable with respect to fluctuations along the transverse directions (y and z). This instability can be suppressed in experiments by squeezing the condensate in the transverse direction, as the cigar-shaped traps do [10].

III. RESULTS AND DISCUSSION: DARK SOLITONS IN HARMONIC TRAPS

We consider BECs confined by harmonic potentials $V_{ext}(x,y,z) = \frac{1}{2} m(\omega_x x^2 + \omega_\perp (y^2 + z^2))$, focusing on elongated geometries of the system along the x-direction. These geometries are experimentally accesible by using large harmonic frequencies along the transverse y–z plane. In what follows, we assume a transverse isotropic trapping of angular frequency $\omega_\perp >> \omega_x$, so that the transverse degrees of freedom are frozen, and the system shows effective 1D dynamics along the x-direction. As a consequence, the interaction strength entering the GP equation has to be renormalized to [3]

$$g = \frac{\hbar^2}{m} \frac{2a}{a_\perp^2} \qquad (10)$$

where $a_\perp$ is the characteristic length of the transverse harmonic oscillator.

We start by characterising the different states we are dealing with, namely solitonic and ground states in 1D harmonic traps. To obtain these states we solve the GP Eq. (1) by using a finite-difference method for the space discretization along with a norm preserving time evolution scheme. The stationary states are reached after an imaginary time evolution. In the soliton case, our initial state contains a node at $x = 0$.
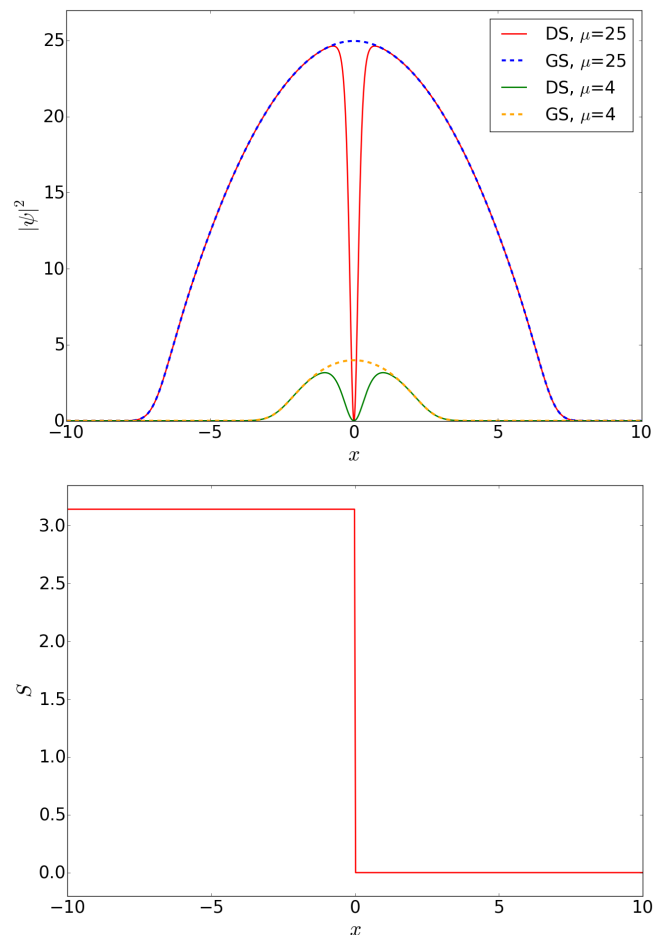

FIG. 2: Top panel: density profiles of dark solitons (DS) and ground states (GS) in a harmonic trap. Bottom panel: phase profiles of dark solitons. All the quantities are expressed in the characteristic units of the harmonic oscillator.

Fig. 2 shows the density profiles (upper panel) of dark solitons and ground states for $\mu = 25 \, \hbar\omega_x$ and $\mu = 4 \, \hbar\omega_x$ and phases (lower panel) for the dark solitons. The phase jump ΔS given by both dark solitons is π, whereas the ground states present a constant phase (not shown) all along the condensates. Confinement plays an important role in the density profile. The first thing to note is that the trap enforces the density to go to zero at the boundary of the condensate. The different chemical potentials considered in Fig. 2 correspond to two different dynamical regimes. For $\mu \gg \hbar\omega_x$ the system enters the so-called Thomas-Fermi regime, where the healing length is very small in comparison with the size of the condensate. On the other hand, for small chemical potentials $\mu \sim \hbar\omega_x$, the system approaches the non-interacting (linear) regime, where the healing length is of the order of the whole condensate. We see that in the trapped system there exists a solitonic state even in the linear case $\mu = \hbar\omega_x$, due the fact that the first excited state of the harmonic oscillator has a node. Therefore the family of solitonic solutions can be considered as the non-linear
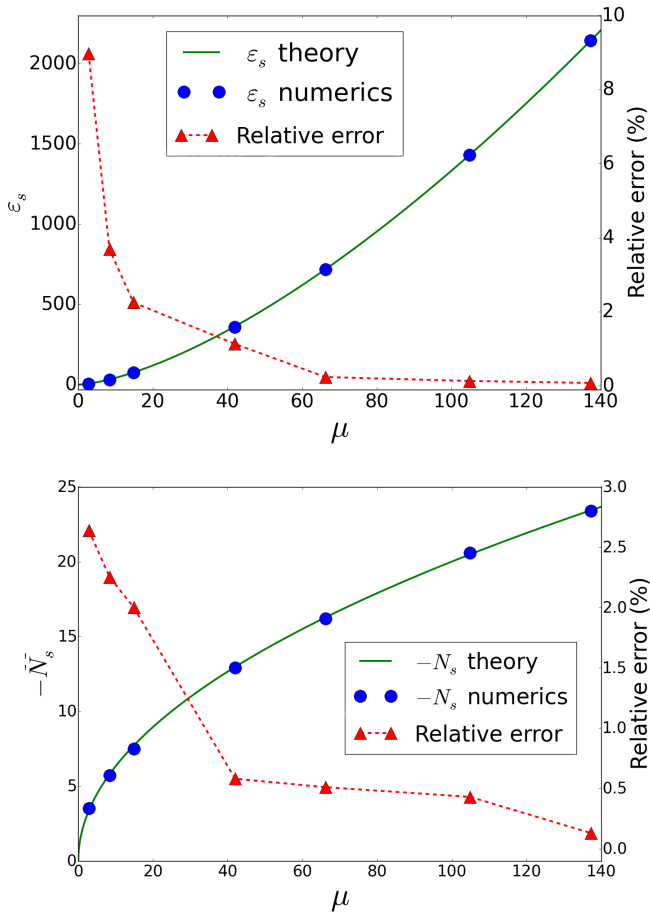
FIG. 3: Energy of the dark soliton (upper panel) and number of particles depleted from the background density due to the presence of the dark soliton (lower panel) as a function of the chemical potential. We also plotted the relative error compared to the analytic case. All the quantities are expressed in the characteristic units of the harmonic oscillator.

continuation of the first linear excited state.

From the previous considerations, we expect that the dark solitons in the Thomas-Fermi regime can be described by the analytical features derived for homogeneous condensates. We expect to have good results when the radius of the condensate is much bigger than the healing length ξ.

A. Excitation energy and missing number of particles

With the aim of comparison with the analytical expressions Eqs. (7, 9), we have evaluated both the excitation energy and the missing number for particles for a trapped soliton, relative to the ground state with the same chemical potential. In the upper panel of Fig. 3 we show our numerical results for the excitation energy of a dark soliton in a harmonic trap. First of all, we can see that the energy follows the functional form given by Eq.(7)

for $v = 0$, increasing as $\propto \mu^{3/2}$. As the chemical potential enters the Thomas-Fermi regime the relative error of the energy, compared with that of the homogenous case, decreases. For μ higher than $60\,\hbar\omega_x$ the discrepancy is lower than 1%. This agrees with the fact that for high chemical potential our trapped system behaves locally as homogeneous.

In the lower panel of Fig. 3 we show our numerical results for the missing number of particles $-N_s$ in our trapped system. We can see that the dependence is in fact $-N_s \propto (\mu/\hbar\omega_x)^{1/2}$. The relative error for $-N_s$ has an analogous behavior to that of the energy. Furthermore, in this case μ needs to be higher than 100 in order to reach a discrepancy lower than 0.5%, reflecting the influence of the boundary conditions on the soliton features for small values of the chemical potential.

B. Oscillatory motion of solitons

Knowing the excitation energy $\varepsilon_s(\mu, v)$ one can derive the equations of motion of a solitary wave in a trapped condensate [11] taking into account that the local density follows from a local chemical potential, that is $(\mu, n) \rightarrow (\mu(x), n(x))$, where $\mu(x) = \mu - \frac{1}{2}m\omega_x^2 x^2$. Requiring the energy to be a constant of motion, and letting x be the position of the soliton, we get

$$0 = \frac{d\varepsilon_s}{dt} = \left(\frac{\partial \varepsilon_s}{\partial \mu}\bigg|_v \frac{d\mu}{dx} + \frac{1}{v}\frac{\partial \varepsilon_s}{\partial v}\bigg|_\mu \frac{\partial v}{\partial t} \right) \dot{x} , \qquad (11)$$

where we arrive at Newton's equation of motion in the form

$$M_{\text{in}}\ddot{x} = -M_{\text{ph}}\omega_x^2 x , \qquad (12)$$

where M_{in} is the inertial mass defined by

$$M_{\text{in}} = \frac{1}{v}\frac{\partial \varepsilon_s}{\partial v}\bigg|_\mu = -\frac{4\hbar m}{g}\left(\frac{\mu}{m} - v^2\right)^{1/2} , \qquad (13)$$

and M_{ph} is the physical mass of the soliton (associated to the missing number of particles $M_{\text{ph}} = mN_s$):

$$M_{\text{ph}} = -m\frac{\partial \varepsilon_s}{\partial \mu}\bigg|_v = -\frac{2\hbar m}{g}\left(\frac{\mu}{m} - v^2\right)^{1/2} . \qquad (14)$$

One can finally obtain that $x(t) \propto \cos(\Omega t)$ with

$$\frac{\omega_x^2}{\Omega^2} = \frac{M_{\text{in}}}{M_{\text{ph}}} = 2 \qquad (15)$$

Such harmonic oscillations have already been observed in experiments, and the frequency ratio measured for dark solitons is $\Omega = \omega_x/\sqrt{2}$ [12] in Bose-Einstein condensates.

In order to check the theoretical predictions, we have performed numerical simulations with the GP Eq. (1) following the real time evolution of a dark soliton imprinted at an off-center location in the trapped condensate. We
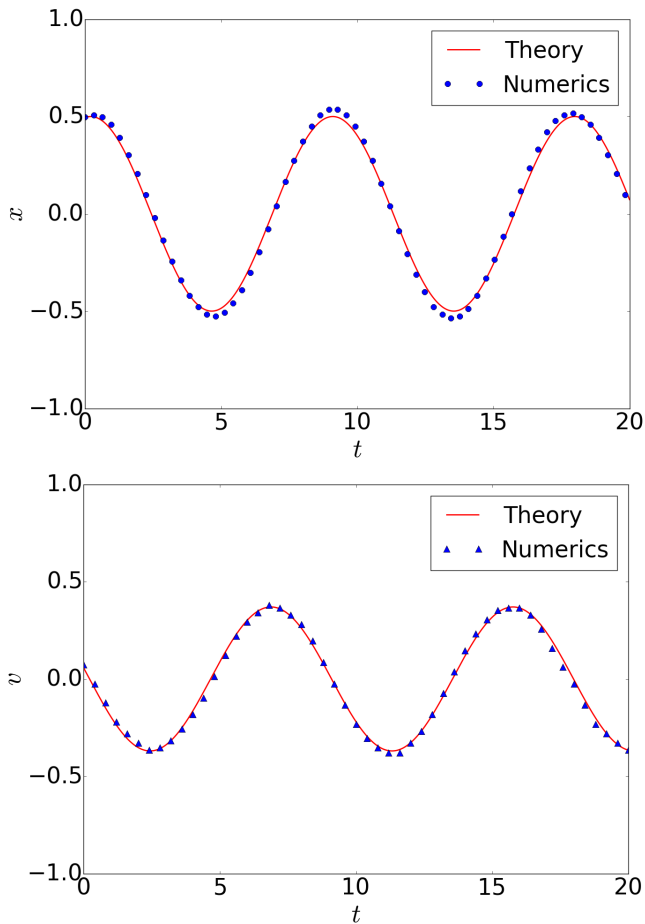
the soliton position.

Figure 4 shows our numerical results for the position (points, upper panel) and velocity (triangles, lower panel) of a soliton in a condensate with $\mu = 100\,\hbar\omega_x$. One can see that the motion of the dark soliton in the trap fits the theoretical values obtained from the expressions for the homogeneous case (solid lines). We note that besides the soliton there is also noise and sound excitations, which are difficult to avoid, in the trap. At same time a slight vibration of the whole condensate condensate is taking place. Because of these reasons our numerical results do not fit perfectly to the theoretical ones.

IV. CONCLUSIONS

We have analyzed the dynamical properties of dark solitons in 1D BECs confined in harmonic potentials. Our numerical results, obtained with the 1D Gross-Pitaeskii equation, show that these solitonic waves share the analytical features derived for homogeneous systems only within the Thomas-Fermi regime, where the size of the condensate is much larger than the characteristic length of the soliton, and the local density approximation applies. In addition, we have demonstrated that the oscillatory motion of a dark soliton in a harmonic trap of angular frequency ω_x follows that of a classical particle in an equivalent trap of frequency $\omega_x/\sqrt{2}$.

FIG. 4: Position (upper panel) and velocity (lower panel) of a soliton in a harmonic trap against time. The analytical predictions $x(t) \propto \cos(\omega_x t/\sqrt{2})$ and $v(t) \propto \sin(\omega_x t/\sqrt{2})$ are also plotted for comparison purposes. All the quantities are expressed in the characteristic units of the harmonic oscillator.

have added white noise to make the simulation more realistic. We observe the subsequent evolution and track

[1] A. Griffin, D. W. Snoke, and S. Stringari, *Bose-Einstein Condensation* Cambridge University Press (1995)
[2] M. H. Anderson, J. R. Ensher, M. R. Matthews, C. E. Wieman, and E. A. Cornell, *Observation of Bose-Einstein Condensation in a Dilute Atomic Vapour* Science **269**, 198 (1995)
[3] F. Dalfovo, S. Giorgini, L. P. Pitaevskii, and S. Stringari, *Theory of Bose-Einstein condensation in trapped gases* Rev. Mod. Phys. **71**, 463 (1999)
[4] C.J. Pethick and H. Smith, *Bose-Einstein Condensation in Dilute Gases* Cambridge University Press (2002)
[5] P. G. Drazin and R. S. Johnson, *Solitons: an introduction* Cambridge University Press (1989)
[6] L. Khaykovich et al. *Formation of a matter-wave bright soliton* Science **296**, 1290 (2002)

[7] T. Tsuzuki, J. Low Temp. Phys. **4**, 441 (1971)
[8] N. D. Mermin, *The topological theory of defects in ordered media* Rev. Mod. Phys. **51**, 591 (1979)
[9] R. G. Scott, F. Dalfovo, L. P. Pitaevskii, and S. Stringari, Phys. Rev. Lett. **106**, 185301 (2011).
[10] S. Burger et al., *Dark solitons in Bose-Einstein Condensates* Phys. Rev. Lett. **83**, 5198 (1999)
[11] V. Konotop and L. Pitaevskii, *Landau dynamics of a grey soliton in a trapped condensate* Phys. Rev. Lett. **93**, 240 (2004)
[12] C. Becker et al., *Oscillations and interactions of dark and darkbright solitons in Bose-Einstein condensates* Nat. Phys. **6**, 496 (2008)

Barcelona, June 2016